Redox Biology 41 (2021) 101946

Contents lists available at ScienceDirect

Redox Biology

journal homepage: www.elsevier.com/locate/redox

Macrophage migration inhibitory factor (MIF) enhances hypochlorous acid production in phagocytic neutrophils

Lisa Schindler [a,b], Leon C.D. Smyth [b], Jürgen Bernhagen [a,c,d,**], Mark B. Hampton [b], Nina Dickerhof [b,*]

[a] Division of Vascular Biology, Institute for Stroke and Dementia Research (ISD), Ludwig-Maximilians-University (LMU), Munich, Germany
[b] Centre for Free Radical Research, Department of Pathology and Biomedical Science, University of Otago, Christchurch, New Zealand
[c] Munich Cluster for Systems Neurology (SyNergy), Munich, Germany
[d] Munich Heart Alliance, German Centre for Cardiovascular Diseases, Munich, Germany

ARTICLE INFO

Keywords:
Neutrophil priming
Phagocytosis
Oxidative stress
Superoxide
NETs
Cytokine

ABSTRACT

Background: Macrophage migration inhibitory factor (MIF) is an important immuno-regulatory cytokine and is elevated in inflammatory conditions. Neutrophils are the first immune cells to migrate to sites of infection and inflammation, where they generate, among other mediators, the potent oxidant hypochlorous acid (HOCl). Here, we investigated the impact of MIF on HOCl production in neutrophils in response to phagocytic stimuli.

Methods: Production of HOCl during phagocytosis of zymosan was determined using the specific fluorescent probe R19-S in combination with flow cytometry and live cell microscopy. The rate of phagocytosis was monitored using fluorescently-labeled zymosan. Alternatively, HOCl production was assessed during phagocytosis of *Pseudomonas aeruginosa* by measuring the oxidation of bacterial glutathione to the HOCl-specific product glutathione sulfonamide. Formation of neutrophil extracellular traps (NETs), an oxidant-dependent process, was quantified using a SYTOX Green plate assay.

Results: Exposure of human neutrophils to MIF doubled the proportion of neutrophils producing HOCl during early stages of zymosan phagocytosis, and the concentration of HOCl produced was greater. During phagocytosis of *P. aeruginosa*, a greater fraction of bacterial glutathione was oxidized to glutathione sulfonamide in MIF-treated compared to control neutrophils. The ability of MIF to increase neutrophil HOCl production was independent of the rate of phagocytosis and could be blocked by the MIF inhibitor 4-IPP. Neutrophils pre-treated with MIF produced more NETs than control cells in response to PMA.

Conclusion: Our results suggest a role for MIF in potentiating HOCl production in neutrophils in response to phagocytic stimuli. We propose that this newly discovered activity of MIF contributes to its role in mediating the inflammatory response and enhances host defence.

1. Introduction

Macrophage migration inhibitory factor (MIF) is an important immune regulator [1]. The name refers to its historic discovery as a T-lymphocyte-derived factor that retains macrophages at sites of inflammation by preventing their random migration [2,3], but belies its various biological activities discovered over the last 25 years. MIF displays proinflammatory (induction of inflammatory cytokines, nitric oxide and matrix metalloproteinases; overriding of immuno-suppressive glucocorticoids) [1,4,5], anti-apoptotic [6], pro-angiogenic [7] and

Abbreviations: ARDS, acute respiratory distress syndrome; BSA, bovine serum albumin; DAMPs, damage-associated molecular patterns; FCS, fetal calf serum; FITC, fluorescein-5-isothiocyanate; fMLP, N-formyl-Met-Leu-Phe; GSA, glutathione sulfonamide; GSH, reduced glutathione; GSSG, glutathione disulfide; GSSX, glutathione present as a disulfide with other low molecular weight thiols; 4-IPP, 4-iodo-6-phenylpyrimidine; LPS, lipopolysaccharide; LTB_4, leukotriene B_4; MIF, macrophage migration inhibitory factor; MPO, myeloperoxidase; NE, neutrophil elastase; NETs, neutrophil extracellular traps; NOX2, NADPH oxidase 2; OpZ, opsonized zymosan; PAF, platelet-activating-factor; PKC, protein kinase C; PLA2, phospholipase A2; PMA, phorbol 12-myristane 13-acetate; SOD, superoxide dismutase.

* Corresponding author. Centre for Free Radical Research, University of Otago, P.O. Box 4345, Christchurch 8140, New Zealand.
** Corresponding author. Institute for Stroke and Dementia Research (ISD), LMU University Hospital, Ludwig-Maximilians-University (LMU) Munich, Feodor-Lynen-Straße 17, 81377 Munich, Germany.
E-mail addresses: juergen.bernhagen@med.uni-muenchen.de (J. Bernhagen), nina.dickerhof@otago.ac.nz (N. Dickerhof).

https://doi.org/10.1016/j.redox.2021.101946
Received 24 February 2021; Received in revised form 11 March 2021; Accepted 12 March 2021
Available online 30 March 2021

pro-proliferative functions [8]. Given its multi-tasking potential, MIF is now recognised as an atypical chemokine [9]. MIF also has an enzymatic tautomerase activity of unknown biological significance, which is facilitated by the protein's unique nucleophilic *N*-terminal proline [10]. The cellular source of MIF is not confined to T lymphocytes, but other immune cells including monocytes/macrophages [11], neutrophils [12], as well as epithelial cells [13], endothelial cells [14], smooth muscle cells [15], and the pituitary gland [16] all express and secrete MIF in response to inflammatory stimuli. MIF is implicated in acute and chronic inflammatory diseases such as septic shock, acute respiratory distress syndrome (ARDS), and rheumatoid arthritis [16–20]. It also drives tumorigenesis and atherogenesis [21,22]. Anti-MIF strategies are therefore an attractive target for ameliorating disease [23–25].

A large body of literature has focused on the interplay between MIF and its effector cells including monocytes, macrophages, T lymphocytes, endothelial cells, fibroblasts, cardiomyocytes, and various tumor cells. Surprisingly, the effect of MIF on the most abundant circulating leukocytes, neutrophils, has not been extensively studied, even though these cells are the first to arrive at sites of inflammation and infection. It is known that MIF acts as a chemoattractant for neutrophils [26–28] and delays their apoptosis [29]. We have recently shown that the ability of MIF to inhibit neutrophil apoptosis is mediated by an indirect mechanism involving the release of pro-survival mediators from peripheral blood mononuclear cells [30]. Investigations into whether MIF can directly impact neutrophil functions, in particular phagocytic and oxidative activities, are warranted.

The ability to ingest bacteria and fungi into phagosomes and produce antimicrobial oxidants are an integral part of the neutrophil's defensive arsenal against invading pathogens. More recently, neutrophil phagocytosis has been shown to play a role in sterile inflammation, i.e. in facilitating the removal of necrotic cellular debris [31,32]. Chief among the antimicrobial oxidants produced inside the neutrophil phagosome is hypochlorous acid (HOCl). HOCl production requires the assembly of the NADPH oxidase 2 (NOX2) on the membrane leading to the generation of superoxide ($O_2^{\cdot-}$) [33]. Myeloperoxidase (MPO) is released into the phagosome from intracellular granules, and at high concentrations it converts superoxide to hydrogen peroxide [34], then uses the hydrogen peroxide to oxidize halides to the corresponding hypohalous acids [35]. The amount of HOCl produced following pathogen ingestion is sufficient to kill some bacteria [36], but not others [37].

To ensure efficient pathogen clearance, neutrophil oxidant production can be amplified by inflammatory mediators in a process called 'priming'. While priming agents do not induce an oxidative response in neutrophils themselves, they can elicit an enhanced oxidant production following exposure to a second activating stimulus. Superoxide production can be primed by cytokines (TNF-α, GM-CSF) [38–41], Toll-like receptor agonists (LPS, flagellin, CL097) [42–44] and chemoattractants (CXCL-8; complement component C5a; leukotriene B_4, LTB_4; platelet activating factor, PAF) [45–49]. In the case of TNF-α [50] and GM-CSF [51], exposure to these cytokines was also demonstrated to enhance MPO-H_2O_2 halide activity in neutrophils.

MIF was reported to augment superoxide production in human neutrophils in response to fMLP as measured by the reduction of cytochrome C [52]. The use of non-specific oxidant probes luminol and rhodamine also demonstrated that exogenously added MIF can increase the oxidative activity of neutrophils stimulated with *Pseudomonas aeruginosa* and anti-neutrophil cytoplasmic antibodies (ANCAs), respectively [53,54]. While these studies collectively suggest a role for MIF in affecting the neutrophil oxidative burst, it is currently unknown whether MIF enhances the production of the most toxic oxidant HOCl in response to phagocytic stimuli, and if so, whether this can be inhibited by small molecule MIF inhibitors.

Studying the impact of MIF on neutrophil oxidant production is not only important for understanding its involvement in regulating microbial killing in the phagosome, but also other oxidant-dependent processes such as neutrophil extracellular trap (NET) formation, cytokine production and cell death [55–57]. The release of NETs, structures of DNA and histones decorated with antimicrobial proteins including MPO, aid in the extracellular clearance of pathogens. However, mounting evidence also suggests that NETs, like MIF, play a detrimental role in ARDS, cancer and cardiovascular disease [58–60]. Interestingly, MIF was found to be important for NET formation in response to *P. aeruginosa* as neutrophils from *Mif* knockout mice and neutrophils treated with an MIF inhibitor showed diminished NET release [53]. Whether exogenous MIF leads to increased NET formation is currently unknown.

The aim of this study was to investigate the effect of MIF on phagosomal neutrophil HOCl production using the HOCl-specific probes R19-S and bacterial glutathione sulfonamide [36,61,62]. Furthermore, we examined whether MIF can enhance oxidant-dependent NET production.

2. Material and Methods

2.1. Reagents

Dextran from *Leuconostoc mesenteroides* (av. mol. wt. 150,000, Sigma, Merck, Darmstadt), Ficoll-Paque and endotoxin-free water (GE Healthcare, Chicago, IL, USA) were used for neutrophil isolation. Cells were cultured in RPMI 1640 media supplemented with 1 mM glutamine (Gibco, Thermo Fisher Scientific, Watham, MA, USA) or in Hank's balanced salt solution (HBSS, Sigma), supplemented with or without heat-inactivated fetal calf serum (FCS) from Sigma. Catalase from bovine liver, cytochrome C from equine heart, superoxide dismutase from bovine erythrocytes, zymosan from *Saccharomyces cerevisiae* and phorbol 12-myristane 13-acetate (PMA), polymyxin B sulphate salt, N-formyl-Met-Leu-Phe (fMLP) were all purchased from Sigma Aldrich. R19-S was synthesized as described [63] and stock solutions (1 mM in acetonitrile) were prepared weekly measuring absorbance at 308 nm (ε_{308} 14000 $M^{-1}cm^{-1}$). 4-Iodo-6-phenylpyrimidine (4-IPP; Santa Cruz Biotechnology) was purchased from Bio-Strategy (Auckland, New Zealand). SYTOX Green nucleic acid stain was purchased from Thermo Fisher Scientific. Monoclonal mouse IgG_1 anti-NE antibody (Clone #950317) was purchased from R&D Systems (Minnaeapolis, MN, USA) and goat anti-mouse Alexa Fluor-647 (AF647) was purchased from Thermo Fischer Scientific. Fluorescein-5-isothiocyanate (FITC) was from Life Technologies (Carlsbad, CA, USA). CELTONE Complete Medium (^{13}C, 98%+) and heavy-labeled glutathione (GSH, $^{13}C_2$+^{15}N) were obtained from Cambridge Isotopes Laboratories (Tewksbury, MA, USA). Hypochlorous acid ($\varepsilon_{292} = 350\ M^{-1}\ cm^{-1}$ at pH 12 [64]) was purchased as commercial chlorine bleach from Pental (Melbourne, Australia).

2.2. Isolation of neutrophils from peripheral blood

Blood for neutrophil isolation was obtained from healthy human volunteers with informed consent and with ethical approval from the Southern Health & Disability Ethics Committee, New Zealand and the Ethics Committee of LMU Munich, Germany. Our protocols for obtaining blood abide by the Declaration of Helsinki principles. Human neutrophil granulocytes were isolated from freshly drawn heparinized blood under sterile conditions. Dextran sedimentation of erythrocytes was followed by a density gradient centrifugation using Ficoll. The intermediate layer containing the PBMC was removed. Neutrophils were isolated from the Ficoll pellet by lysing erythrocytes in hypotonic buffer [65]. Neutrophils were resuspended in RMPI supplemented with 10% heat-inactivated FCS (v/v). Purity (98–99%) was verified using flow cytometry analysis using the characteristic forward/side scatter. Serum was obtained from blood collected without anticoagulant and left to clot at room temperature. The clot was pelleted (1200×g; 2 min) and the serum was collected and stored on ice until required.

2.3. Expression and purification of recombinant human MIF and preparation of oxMIF

Recombinant human MIF was expressed in an *Escherichia coli* BL-21-based system and purified using the protocols described before [66,67]. The concentration of LPS in the MIF preparation was measured using the limulus amoebocyte assay (LAL, Lonza, Cologne, Germany), following the manufacturer's instructions, and was <0.02–0.1 ng/μg MIF. MIF was treated with a 5-fold molar excess of HOCl to generate 'oxMIF' as described before, which results in oxidation of the *N*-terminal proline to a proline imine [66].

2.4. Preparation of zymosan particles

Zymosan A (from *S. cerevisiae,* 5 mg/ml = 3×10^8 particles/ml) was suspended in PBS at 20 mg/ml, sonicated for 5 min, boiled for 10 min, and washed twice by centrifugation at 4000×*g* before being resuspended in PBS (20 mg/ml) and frozen in aliquots at -20 °C. For FITC labeling, zymosan particles were pelleted by centrifugation and resuspended in 0.1 M sodium carbonate buffer, pH 9, before sonicating in a water bath for 2 min. FITC (1 mg/ml in DMSO) was added at a final concentration of 30 μg/ml, incubated at 37 °C in the dark for 30 min and washed twice with HBSS. For opsonization prior to phagocytosis by neutrophils, labeled and non-labeled zymosan was incubated with 50% autologous serum for 30 min at 37 °C, washed twice, resuspended in HBSS and stored on ice until further use.

2.5. Measuring HOCl production in neutrophils phagocytosing zymosan using R19-S and flow cytometry or live cell fluorescence microscopy

Nonfluorescent R19-S is oxidized to the red fluorescent rhodamine 19 (R19) by HOCl and can be used to monitor HOCl production in neutrophils using live cell imaging or FACS analysis as described before [62,63]. Neutrophils (1×10^7/ml) were incubated with MIF or oxMIF (10 μg/ml) and 30 μg/ml of LPS-scavenger polymyxin B in RPMI with 10% FCS for 60 min with end-over-end rotation at 37 °C. Cells were pelleted and resuspended in HBSS.

For FACS analysis, neutrophils were diluted to 1×10^6 cells/ml in HBSS, 10 μM of R19-S was added and incubated for 5 min at 37 °C before opsonized zymosan (5×10^6/ml) was added and incubated with end-over-end rotation. Red fluorescence intensity (Ex_{488}/Em_{575}) of the neutrophil population was measured at 5, 10, 15 and 30 min using an FC500 MPL flow cytometer (Beckman Coulter).

For live cell imaging of R19 fluorescence, neutrophils were diluted to 1×10^6 cells/ml in HBSS after pre-incubation with MIF, then chilled on ice for 30 min, R19-S (10 μM), methionine (1 mM) and FITC-labeled or unlabeled opsonized zymosan (1×10^7/ml) were added and cell suspensions were transferred to a 96- well clear bottom plate (100 μl/well). The plate was centrifuged at 200×*g* for 1 min and placed into an Olympus IX81 fluorescent microscope pre-heated to 37 °C. Time lapse images (frames) of Cy3 and DIC channels were taken every 18 s and of Cy3, DIC and FITC channels every 30 s when using non-labeled zymosan and FITC-labeled zymosan, respectively, over 60 min with a 20x objective. CellProfiler (Image J v 3.1.8) was used to quantify the fluorescence signal of single cells and intensity over time. Briefly, neutrophils were identified in the DIC channel, then FITC-positive particles within the cell mask classified as phagosomes. The R19-S intensity within neutrophils and phagosomes was measured, and these were classed positive or negative depending on signal intensity (Supplementary Figure 1). When analysing FITC-zymosan particles per cell, the value recorded at the first time-point was subtracted from all other time points in order to remove any signal stemming from non-phagocytosed particles.

2.6. Monitoring oxidation of bacterial glutathione during neutrophil phagocytosis of Pseudomonas aeruginosa using LC-MS

Oxidation of bacterial glutathione during phagocytosis by human neutrophils was monitored using ^{13}C-labeled *Pseudomonas aeruginosa* and a multiple reaction monitoring (MRM)-based stable isotope dilution liquid chromatography tandem mass spectrometry assay as described before [36]. In brief, *P. aeruginosa* strain PAO1 (ATCC 47085) was stored and grown under standard conditions and maintained on Columbia sheep blood agar plates. For experiments, PAO1 was grown overnight CELTONE Complete ^{13}C Medium at 37 °C, washed with PBS and opsonized with 10% autologous serum in HBSS for 20 min. Neutrophils (2×10^7/ml) were incubated with or without MIF (10 μg/ml) and 30 μg/ml of polymyxin B for 60 min with end-over end rotation at 37 °C before the addition an equal volume of opsonized *P. auruginosa* (2×10^8/ml). After a 5 min incubation at 37 °C with end-over-end rotation, phagocytosis was stopped by the addition of ice-cold PBS. Neutrophils were pelleted by centrifugation at 100*g* for 5 min at 4 °C. Non-phagocytosed bacteria were determined by serially diluting the supernatants in pH 11 water and plating on sheep blood agar plates. To the neutrophil pellet, acetonitrile (50%) and NEM (20 mM) were added and incubated at 60 °C for 15 min. Cell debris and protein was removed by centrifugation at 12,000 g for 5 min and ^{13}C-GSH (as the NEM adduct), ^{13}C-GSSG (glutathione disulfide) and ^{13}C GSA (glutathione sulfonamide) were determined in the supernatant using stable-isotope-dilution LC-MS. GSSX (mixed disulfides of glutathione with other LMW thiols) was determined by determining the GSH concentration following the reduction with DTT and subtracting the GSH and 2x the GSSG concentration measured prior to the addition of DTT. Total glutathione was calculated by [GSH]+2x[GSSG]+[GSSX]+[GSA].

2.7. Measuring superoxide production of PMA- and fMLP-stimulated neutrophils

Superoxide production in neutrophils was monitored by a continuous cytochrome C reduction assay. Neutrophils (5×10^5/ml) were incubated with increasing concentrations of MIF and oxMIF (0, 0.001, 0.01, 0.1, 1, and 10 μg/ml) in RPMI supplemented with 10% heat-inactivated FCS (v/v) and 30 μg/ml of polymyxin B with end-over-end rotation at 37 °C. At various time points (10 min to 4 h), neutrophils were pelleted and resuspended in pre-warmed HBSS. Catalase (20 μg/ml) and cytochrome C (40 μM) were added followed by the addition of fMLP (100 nM) or PMA (100 ng/ml) to induce the oxidative burst. The reduction of cytochrome C (40 μM) by superoxide was measured by monitoring the absorbance at 550 nm every 15 s for 5 min at a slit width of 0.5 nm using a Hitachi spectrophotometer. The rate of absorbance change was determined for the linear part and converted to the rate of superoxide production (nmol superoxide/min/10^6 cells) using $\epsilon = 21.1 \times 10^3$ $M^{-1}cm^{-1}$. To confirm that the absorbance change was superoxide-dependent, SOD (20 μg/ml) was added prior to the addition of stimulant.

In separate experiments, MIF was also incubated with a ten-fold molar excess of the small molecule MIF inhibitor 4-IPP for 15 min at room temperature before adding the proteins to neutrophils.

2.8. Measuring generation of NETs using the SYTOX green plate assay

NET formation by neutrophils was measured using the SYTOX Green plate assay as described before [68]. Neutrophils (1×10^7/ml) were incubated with MIF and oxMIF (10 μg/ml) and 30 μg/ml polymyxin B in RPMI with 10% heat-inactivated FCS (v/v) for 60 min at 37 °C, cells were pelleted and resuspended in HBSS. Cells were diluted into HBSS to a final concentration of 1×10^6 cells/ml and 100 μl was added to a 96-well plate in quadruplicates before adding 20 nM PMA to induce NET formation. SYTOX Green (30 nM) was added at various time points and green fluorescence was measured using a PolarStar fluorescence plate

reader (Ex_{485}, Em_{520}). Background signal from a sample containing MIF alone was subtracted. To test whether MIF itself could induce NET formation, neutrophils were incubated with MIF without adding PMA.

NET formation was confirmed using fluorescence microscopy staining extracellular DNA and neutrophil elastase. For this, neutrophils (1×10^7/ml) were pre-incubated in the presence or absence of 10 μg/ml MIF or oxMIF for 60 min in RPMI supplemented with 10% heat-inactivated FCS (v/v) and 30 μg/ml polymyxin B at 37 °C. Cells were added at a concentration of 5×10^6 cells/ml to a 24-well plate on a coverslip in HBSS, PMA (20 nM) was added and incubated at 37 °C for 4 h. Paraformaldehyde was carefully added into each well at a final concentration of 4% and incubated for 20 min at room temperature. Each sample was then washed with PBS four times and 0.5% Triton X-100 in PBS was added to permeabilize the cells for 10 min, followed by another three washing steps. Each sample was blocked with 10% BSA/PBS for 1 h at 37 °C, before a monoclonal mouse IgG_1 anti-NE antibody (Clone #950317) was added at a concentration of 1:500 in 3% BSA/PBS for 1 h at 37 °C. Next, samples were washed and the secondary antibody (goat anti-mouse AF647) was added at a concentration of 1:500 in 3% BSA/PBS for 1 h at 37 °C, followed by another washing step. In addition, SYTOX Green was added to each sample at a final concentration of 200 nM and incubated in the dark for 5 min at RT. At the end, each coverslip was placed face down on a small drop of Fluormount G and left to dry. Neutrophil elastase and SYTOX Green signals were analyzed using Leica LasX fluorescent microscope and images of Cy5 (NE), DIC and FITC (SYTOX Green) channels were taken with a 40x objective.

2.9. Statistical analyses

Graphs were plotted and statistical analysis was performed using GraphPad Prism 8 (GraphPad Software, La Jolla, Ca, USA). Differences between groups were determined by one-way ANOVA or student's t-test. A p-value <0.05 was considered significant.

3. Results

3.1. MIF enhances HOCl production in neutrophils phagocytosing opsonized zymosan

The HOCl-sensitive fluorescent probe R19-S was used in combination with flow cytometry to measure HOCl production in neutrophils phagocytosing opsonized zymosan. Fig. 1A shows a representative histogram for neutrophils developing red fluorescence as a result of HOCl-mediated oxidation of R19-S. When neutrophils were pre-incubated with MIF prior to the addition of zymosan, red R19 fluorescence developed more rapidly compared to control cells, indicated by a larger proportion of red fluorescent neutrophils at early time points (Fig. 1B). At 5 and 10 min, 2.2 and 1.2 times as many neutrophils, respectively, were fluorescence-positive in the MIF-treated group than in the control group. After 15 min, the number of fluorescence-positive cells reached a

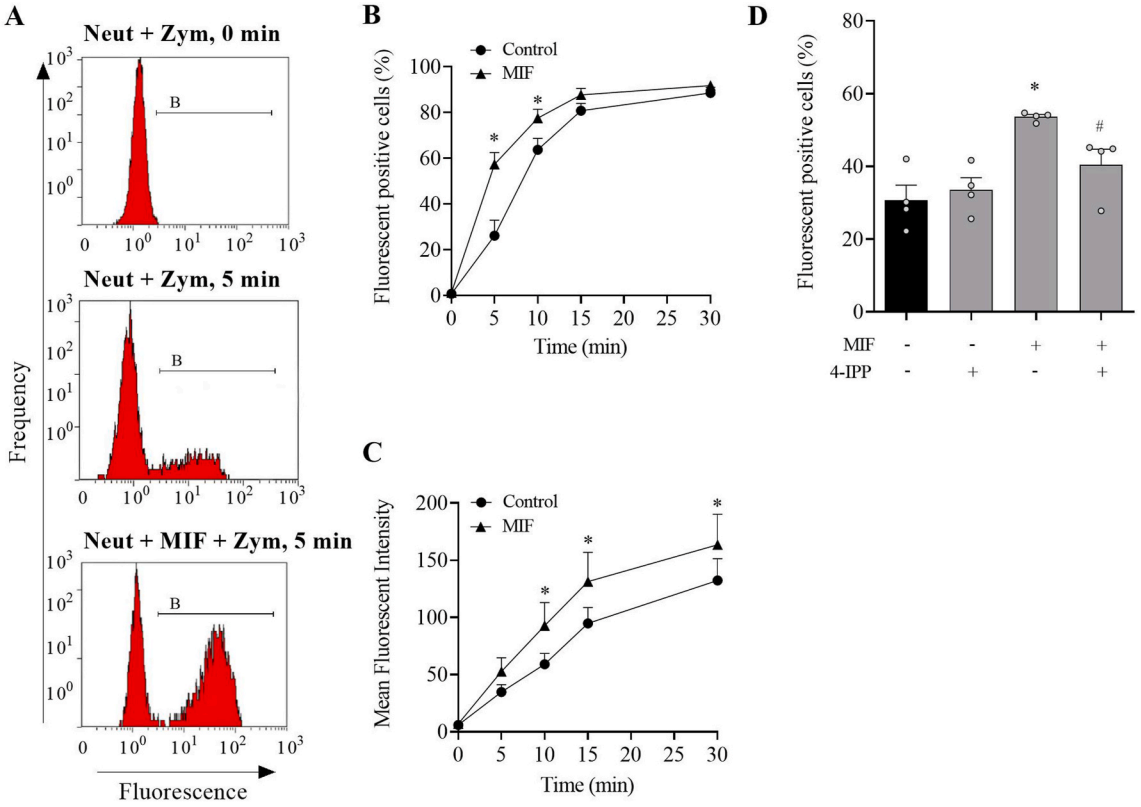

Fig. 1. MIF increases HOCl production in neutrophils phagocytosing zymosan. Neutrophils (Neut, 1×10^6/ml), which were pre-incubated with and without MIF (10 μg/ml) for 1 h, were incubated with opsonized zymosan (Zym, 5×10^6/ml) with end-over-end rotation at 37 °C in the presence of R19-S (10 μM). Red fluorescence of the HOCl-specific product R19 was measured after 0, 5, 10, 15 and 30 min. (**A**) Representative flow cytometry data after 0 and 5 min with the red R19 fluorescence represented as histograms. (**B**) The proportion of cells positive for red fluorescence as a percentage of total gated neutrophils and **(C)** the mean fluorescence intensity for the fluorescent population 'B' was plotted. Data are presented as mean ± SEM for four independent experiments using different blood donors. Statistical difference to the control was determined using repeated-measures two-way ANOVA with Sidak's multiple comparison test and is indicated by *$p<0.05$. (**D**) MIF was treated with a ten-fold molar excess of 4-IPP for 15 min at RT before adding to neutrophils and percentage of fluorescent cells was determined after 5 min phagocytosis of zymosan in the presence of R19-S. Each data point represents an independent experiment using a different donor and the bar represents the mean ± SEM. Statistical differences to the control was determined using one-way ANOVA with Holm-Sidak multiple comparison test and is indicated by *$p<0.05$. A statistical difference between MIF and its 4-IPP-treated counterpart was determined using a paired student's t-test and is indicated by #$p<0.05$. (For interpretation of the references to colour in this figure legend, the reader is referred to the Web version of this article.)

maximum of 80% in both MIF-treated and control neutrophils. Furthermore, the mean fluorescence intensity at 5, 10, 15 and 30 min was significantly increased 1.5, 1.6, 1.4 and 1.2-fold in MIF-treated neutrophils consistent with a larger amount of HOCl being produced per neutrophil following exposure to the cytokine (Fig. 1C).

The MIF protein used in the present study was expressed recombinantly in a bacterial expression system and purified by ion-exchange chromatography. To rule out any LPS-mediated effects, we included the LPS-scavenger polymyxin B in all experiments at a concentration that was previously shown to scavenge the levels of LPS present in recombinant MIF preparations [30]. To further verify that the effect on HOCl production was due to MIF itself rather than any remaining traces of bacterial contaminants, we pre-treated MIF with the small molecule inhibitor 4-IPP. MIF pre-treated with the inhibitor did not enhance neutrophil HOCl production, indicating that the effect was MIF-dependent (Fig. 1D).

We also monitored HOCl production in individual neutrophils phagocytosing opsonized zymosan using R19 fluorescence and live cell microscopy (Fig. 2A). In agreement with the flow cytometry results, MIF enhanced HOCl production in neutrophils, as indicated by an increase in both the percentage of cells positive for red R19 fluorescence (Fig. 2B) and the intensity of R19 fluorescence within individual cells during early stages of phagocytosis of zymosan (Fig. 2C).

Next, to investigate whether the MIF-mediated increase in HOCl production was due to an increased rate of phagocytosis, we monitored the ingestion of green fluorescent FITC-labeled zymosan particles by live cell microscopy. The number of green-fluorescent zymosan particles taken up by individual neutrophils was not different between the two groups (Fig. 3A and B, Supplementary Figure 2). To further scrutinize whether MIF enhanced HOCl production independently of a potential effect on phagocytosis, we quantified the number of intracellular green-fluorescent particles that were also positive for red R19 fluorescence, thereby normalizing to the number of ingested particles (Fig. 3C, Supplementary Figure 2). The percentage of zymosan particles that were positive for both green and red fluorescence was increased in MIF-treated neutrophils during early time points, confirming that MIF potentiated HOCl production beyond any effect on the rate of phagocytosis (Fig. 3C, Supplementary Figure 2).

3.2. MIF increases HOCl production in neutrophils phagocytosing *Pseudomonas aeruginosa*

As an alternative method to assess HOCl production in neutrophil phagosomes, we monitored oxidation of bacterial glutathione during phagocytosis of *P. aeruginosa*. When glutathione reacts with HOCl, a proportion of it is oxidized to glutathione sulfonamide (GSA). Unlike disulfides of glutathione, GSA is a product specific to HOCl, and can thus be used as a marker of this oxidant [61]. We have previously shown that during phagocytosis of *P. aeruginosa*, the formation of GSA from bacterial glutathione depended on the activity of MPO and was thus indicative of HOCl reacting with the bacteria [36].

Uptake of *P. aeruginosa* by control and MIF-treated neutrophils was

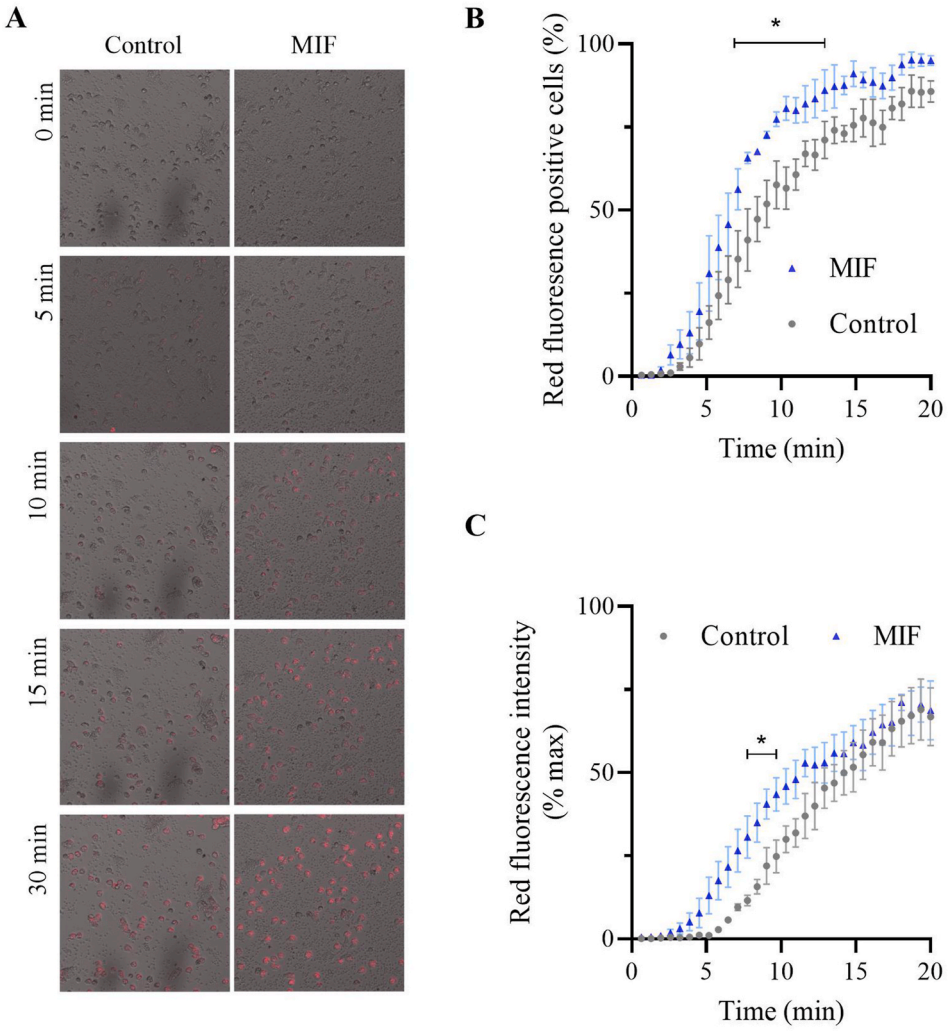

Fig. 2. The effect of MIF on HOCl production of individual neutrophils assessed by live-cell fluorescence microscopy. (**A**) Time-lapse frames after 0, 5, 10, 15 and 30 min from a movie of neutrophils (1×10^6) and neutrophils pre-treated with MIF (10 μg/ml, 1 h) phagocytosing opsonized zymosan (1×10^7/ml) in the presence of R19-S (10 μM). Images show the merge of the Cy3 (red R19 fluorescence) and DIC channels at indicated time points. Representative images of three independent experiments are shown. Image analysis was performed and the (**B**) the percentage of R19-positive cells and (**C**) mean R19 fluorescence intensity as a percentage of the maximal intensity were determined. Mean ± SEM of three independent experiments using different blood donors. Statistical difference to the control was determined using repeated-measures two-way ANOVA with Sidak's multiple comparison test and is indicated by *$p<0.05$ (10.3–20 min in (B) and 7.7–9.7 min in (C)). (For interpretation of the references to colour in this figure legend, the reader is referred to the Web version of this article.)

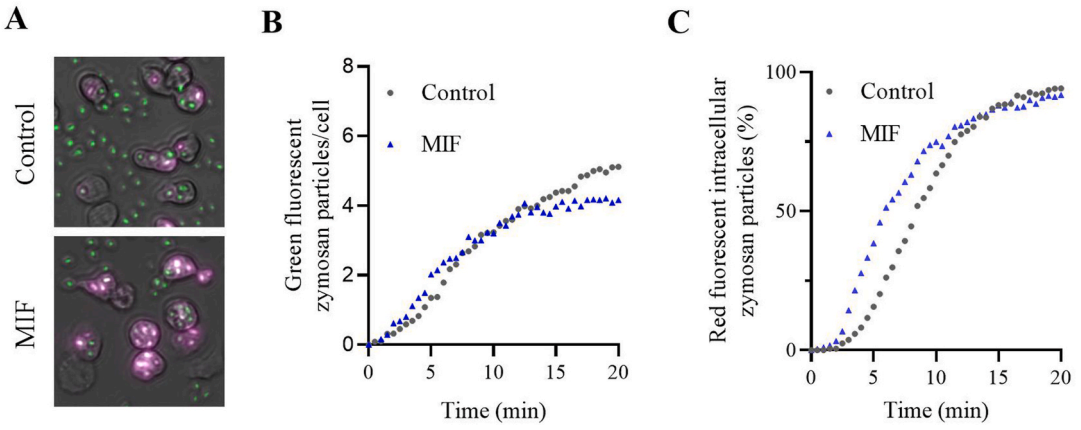

Fig. 3. The effect of MIF on neutrophil phagocytosis FITC-labeled opsonized zymosan (1×10^7/ml) was added to neutrophils (1×10^6/ml), which were pre-incubated with or without 10 μg/ml MIF for 1 h. Phagocytosis of FITC-labeled opsonized zymosan was monitored by live cell microscopy in the presence of R19-S (10 μM). **(A)** A representative time lapse image taken at 15 min is shown with a merge of DIC, Cy3 (R19 fluorescence, purple) and FITC (green) channels; co-localization (white). Image analysis was performed and **(B)** the number of FITC-labeled zymosan particle per cell and **(C)** the percentage of intracellular green fluorescent particles that were also red fluorescent were determined. Representative results of three independent experiments using different blood donors is shown. Results from individual experiments are shown in Supplementary Fig. 2. (For interpretation of the references to colour in this figure legend, the reader is referred to the Web version of this article.)

not significantly different with 95.8±1.6% and 96.0±2.1% (mean ± SEM) of starting bacteria being phagocytosed at 5 min, respectively. The concentration of bacterial GSA was slightly but significantly higher when MIF-treated neutrophils phagocytosed *P. aeruginosa* compared to control neutrophils (3.8 ± 0.3 nM vs 4.6 ± 0.5 nM; mean ± SEM; p = 0.03, paired *t*-test), while all other bacterial glutathione species were not significantly different (Fig. 4A–E). Importantly, the proportion of bacterial glutathione present as glutathione sulfonamide (%GSA, Fig. 4F), which is independent of the number of phagocytosed bacteria, was 30% higher following MIF treatment (7.1 ± 1.0% vs 5.5 ± 0.7%; mean ± SEM; p = 0.02, paired *t*-test).

3.3. MIF increases the rate of superoxide production in neutrophils

We probed whether increased HOCl production in MIF-treated neutrophils was due to an amplification of the NOX2 activity and thus the production of superoxide, an oxidant upstream of HOCl. It is not possible to quantitatively measure superoxide in phagosomes, so the impact of MIF on neutrophil superoxide production was measured in response to the soluble stimuli PMA or fMLP by monitoring the reduction of cytochrome C, indicated by an increase in absorbance at 550 nm. A steeper increase in superoxide was observed when neutrophils were exposed to MIF prior to stimulation (Fig 5A, D). In the case of PMA, MIF also decreased the lag time (Fig. 5A). Superoxide dismutase (SOD)

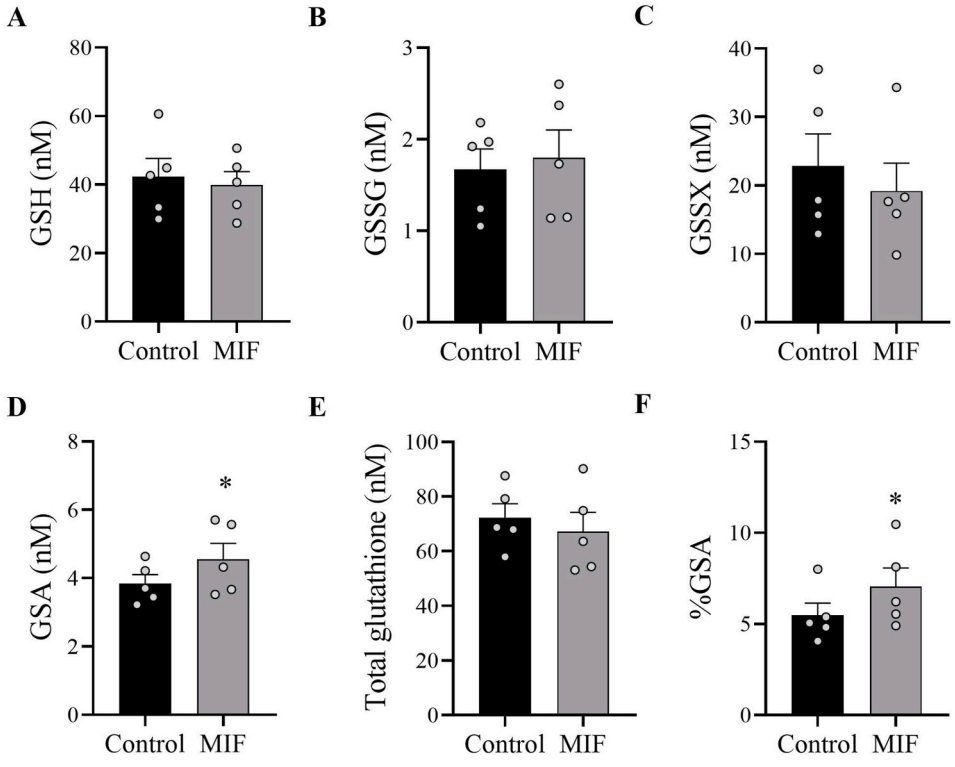

Fig. 4. The effect of MIF on oxidation of bacterial glutathione during phagocytosis by neutrophils. Neutrophils (1×10^7/ml), which were pre-incubated with and without MIF (10 μg/ml) for 1 h, were incubated with ^{13}C-grown *Pseudomonas aeruginosa* (1×10^8/ml) with end-over-end rotation at 37 °C for 5 min. Neutrophils were pelleted by centrifugation and acetonitrile (50%) and NEM (20 mM) were added and incubated at 60 °C for 15 min. Cell debris and protein was removed by centrifugation and **(A)** ^{13}C-GSH (as the NEM adduct), **(B)** ^{13}C-GSSG (glutathione disulfide), **(C)** ^{13}C-GSSX (glutathione present in a mixed disulfide with another low molecular thiol) and **(D)** ^{13}C-GSA (glutathione sulfonamide) were determined in the supernatant using stable-isotope-dilution LC-MS. **(E)** Total glutathione was calculated by [GSH]+2x[GSSG]+[GSSX]+[GSA]. **(F)** GSA was expressed as a percentage of total glutathione. Bars represent means + SEM from independent experiments using different blood donors. A significant difference between control and MIF-treated neutrophils was identified by a paired *t*-test and is indicated by *p<0.05.

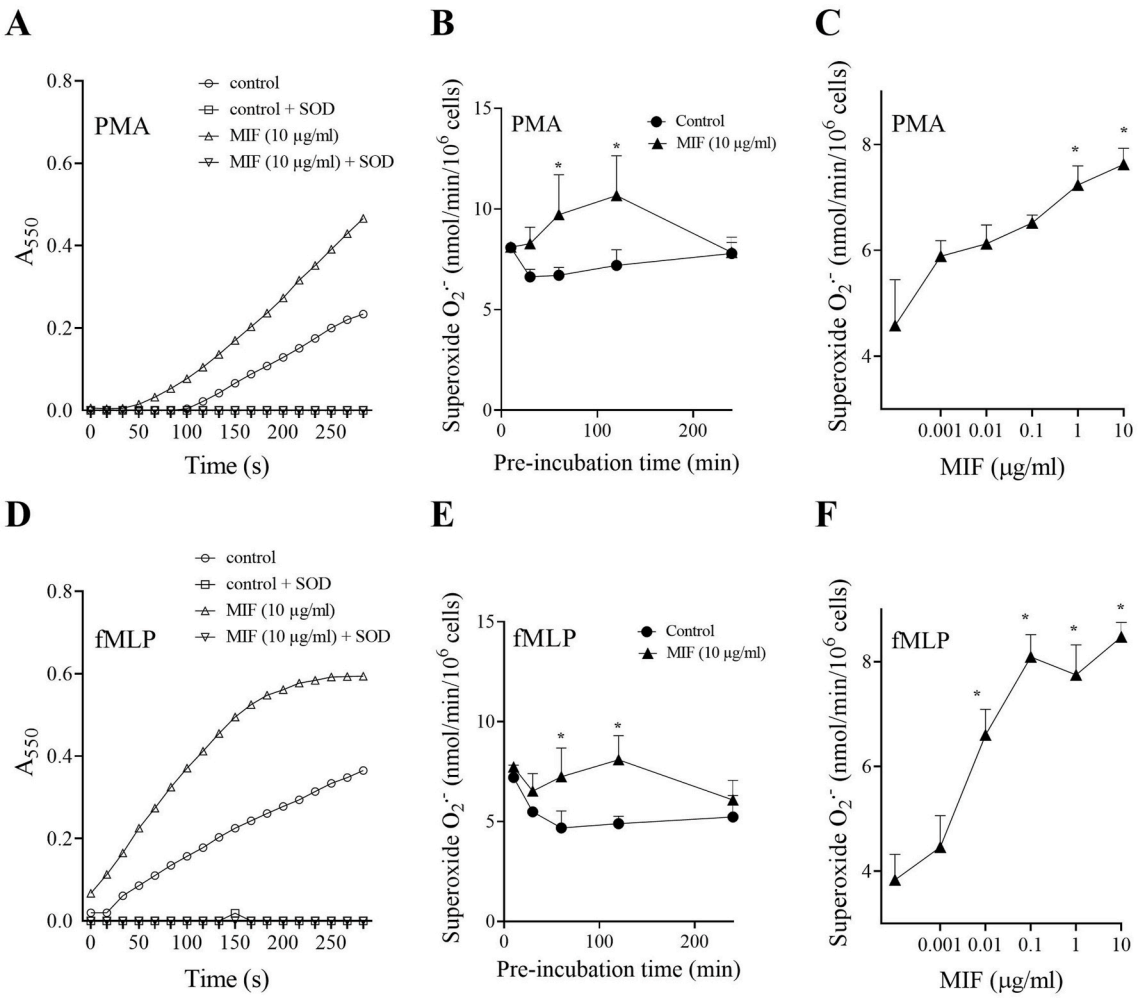

Fig. 5. MIF increases the rate of superoxide production in neutrophils activated by PMA or fMLP. Neutrophils (5×10^5/ml), which were pre-treated with and without of MIF (10 μg/ml) for 1 h, were stimulated with **(A-C)** PMA (100 ng/ml) or **(D-E)** fMLP (100 nM). Superoxide production was assessed by measuring the reduction of cytochrome C as indicated by an increase in absorbance at 550 nm over time. SOD (20 μg/ml) was added to validate that the response was dependent on superoxide. **(A + D)** A representative A_{550} trace recorded after the addition of PMA or fMLP. **(B + E)** Neutrophils were pre-incubated with MIF (10 μg/ml) up to 240 min and superoxide production was measured at indicated time points. The rate of superoxide production was derived from the linear part of the absorbance trace as described in Material and Methods. Data are presented as the mean ± SEM of three independent experiments using different blood donors. A statistical difference to the control was determined using repeated-measures two-way ANOVA with Sidak's multiple comparison test and is indicated by *p<0.05. **(C + F)** Neutrophils were incubated with increasing concentrations of MIF for 1 h before measuring the rate of superoxide production. Data are presented as mean ± SEM of three independent experiments using different blood donors. A statistical difference to the control was determined using one-way ANOVA with Holm-Sidak multiple comparison test and is indicated by *p<0.05.

completely abolished the increase in absorbance in both control and MIF-treated neutrophils confirming that superoxide was responsible for the reduction of cytochrome C. Incubation of neutrophils with MIF alone did not stimulate superoxide production (data not shown).

The rate of superoxide production in response to both PMA and fMLP was greatest shortly after neutrophils were isolated from peripheral blood, and decreased slightly thereafter (Fig. 5B, E). In contrast, when neutrophils were incubated in the presence of MIF, the superoxide production rate was maintained in response to fMLP and even increased in response to PMA for up to 2 h. At 4 h, superoxide production in control and MIF-treated neutrophils was not different.

The effect of MIF on the rate of neutrophil superoxide production was concentration-dependent over the range of 0.001 to 10 μg/ml when PMA was the stimulus (Fig. 5C). When fMLP was used to induce superoxide production, pre-exposure to MIF enhanced the rate at which superoxide was produced in a concentration-dependent manner up to 0.1 μg/ml, with no further increase observed at higher concentrations (Fig. 5F).

Incubation of MIF with 4-IPP before its addition to neutrophils abrogated its ability to enhance superoxide production in neutrophils in response to fMLP (Fig. 6), suggesting that MIF was directly responsible for the observed effect on superoxide generation.

3.4. *Oxidation of the MIF N-terminal proline by HOCl does not affect its ability to increase oxidant and NET production in neutrophils*

We have previously shown that HOCl oxidizes the *N*-terminal proline of MIF to a proline-imine (oxMIF) [66]. While the intrinsic tautomerase activity was abolished in oxMIF, it was still able to stimulate cytokine release from monocytes and inhibit neutrophil apoptosis [30]. Here, we investigated whether the conversion of MIF into oxMIF has any effect on its ability to increase oxidant production in neutrophils (Fig. 7). OxMIF increased HOCl (Fig. 7A) and superoxide (Fig. 7B) production in neutrophils to the same extent as MIF.

3.5. *MIF enhances PMA-induced NET formation*

The generation of reactive oxygen species is known to be important

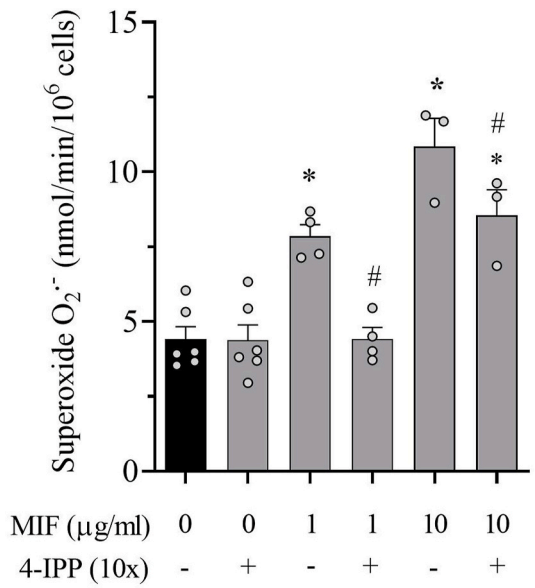

Fig. 6. The effect of small molecule inhibitor 4-IPP on MIF's ability to increase fMLP-induced neutrophil superoxide production. (**A**) MIF was treated with a ten-fold molar excess of 4-IPP for 15 min at room temperature before it was added at either 1 μg/ml or 10 μg/ml to neutrophils (5×10^5/ml). After 1 h incubation, superoxide production was induced by fMLP and measured using the cytochrome C assay described in Fig. 5. Each data point represents an independent experiment using different blood donors and the bar represents the mean ± SEM. Statistical difference to control within each group was determined using one-way ANOVA with Holm-Sidak multiple comparison test and is indicated by *p<0.05. Statistical differences between MIF and its 4-IPP- treated counterpart at a given MIF concentration was determined using a paired student's t-test and is indicated by #p<0.05.

for the production of neutrophil extracellular traps (NETs) by neutrophils [55]. We therefore investigated whether MIF has an effect on neutrophil NET formation using a SYTOX Green fluorescence plate assay as a measure of extracellular DNA. MIF alone was unable to induce NETs over a time course of 4 h (Fig. 8A). However, when PMA was used to stimulate NET formation, pre-treatment with MIF resulted in an increased fluorescence signal compared to that elicited by PMA alone, indicating that MIF enhances or 'primes' NET formation in neutrophils (Fig. 8A). To confirm this finding, fluorescence microscopy was performed to visualize extracellular NETs through co-localization of extracellular DNA and neutrophil elastase and DNA (Fig. 8B). In agreement with the plate assay, neutrophils that had been pre-exposed to MIF showed more NET structures in response to PMA than control cells. Oxidation of MIF by HOCl did not diminish the protein's ability to prime neutrophil NET production (Fig. 8C).

4. Discussion

The present study is the first to show that MIF serves as a priming agent for the HOCl-producing activity of phagocytic neutrophils. Using a combination of live cell microscopy, flow cytometry and mass spectrometry, we demonstrate that while exposure to MIF does not lead to an activation of oxidant production in neutrophils itself, it enhances HOCl production in response to opsonized zymosan and *P. aeruginosa*.

MIF is widely regarded to be a harmful player in disease owing to its pro-inflammatory and tumorigenic activity profile. However, in some settings it is known to be tissue-protective, such as in amyotrophic lateral sclerosis (ALS) and in the early phase of cardiac ischemia/reperfusion injury [69,70]. Furthermore, MIF has recently been reported to be essential for immunity against an intestinal helminth parasite [71]. The present study also suggests a beneficial role for this highly conserved cytokine in host defense. HOCl is the most potent antimicrobial oxidant produced in the neutrophil phagosome. For some bacteria the amount of HOCl that reacts with them inside the neutrophil phagosome is enough to kill them [36], but for others it is insufficient to be solely responsible for microbial death [37,72]. It is conceivable that at the site of inflammation, MIF, like other priming cytokines, is released from macrophages, endothelial cells and neutrophils themselves and acts in a paracrine and autocrine fashion to boost HOCl production in phagocytic neutrophils to ensure efficient killing of invading microorganisms. In the future, it will be of interest to investigate whether MIF improves killing in situations where insuffucient doses of HOCl react with internalized bacteria to kill them, and to determine whether MIF contributes to the capacity of neutrophils to combat microorganisms *in vivo*.

A prerequisite for HOCl generation in neutrophils is the activation of NOX2, which supplies superoxide ($O_2^{\cdot-}$) to the HOCl-producing enzyme MPO. Here, we show that MIF increases NOX2 activity in neutrophils stimulated with fMLP and PMA in a concentration-dependent manner. Consistent with our finding is a previous study that, like us, used the cytochrome C reduction assay to reveal augmented fMLP-induced superoxide production following incubation with comparable levels of MIF

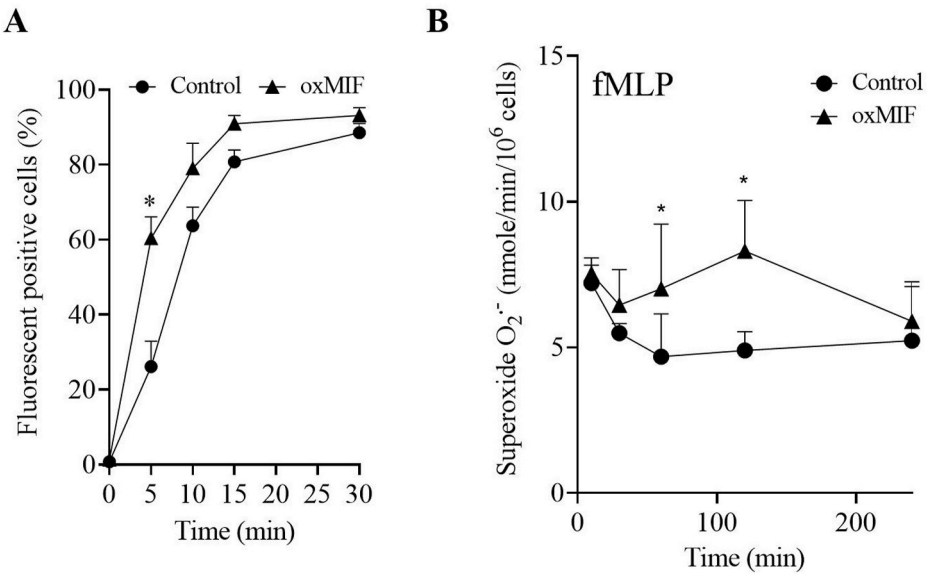

Fig. 7. Oxidation of the MIF *N*-terminal proline by HOCl does not affect its ability to increase oxidant production in neutrophils. MIF was oxidized with a five-fold molar excess of HOCl (oxMIF) before adding the protein to neutrophils at a concentration of 10 μg/ml, incubating for 1 h and measuring **(A)** the proportion of red fluorescence-positive cells during phagocytosis of zymosan in the presence of R19-S using FACs analysis as described in Fig. 1, **(B)** the production of superoxide in response to fMLP using the cytochrome C reduction assay described in Fig. 5.

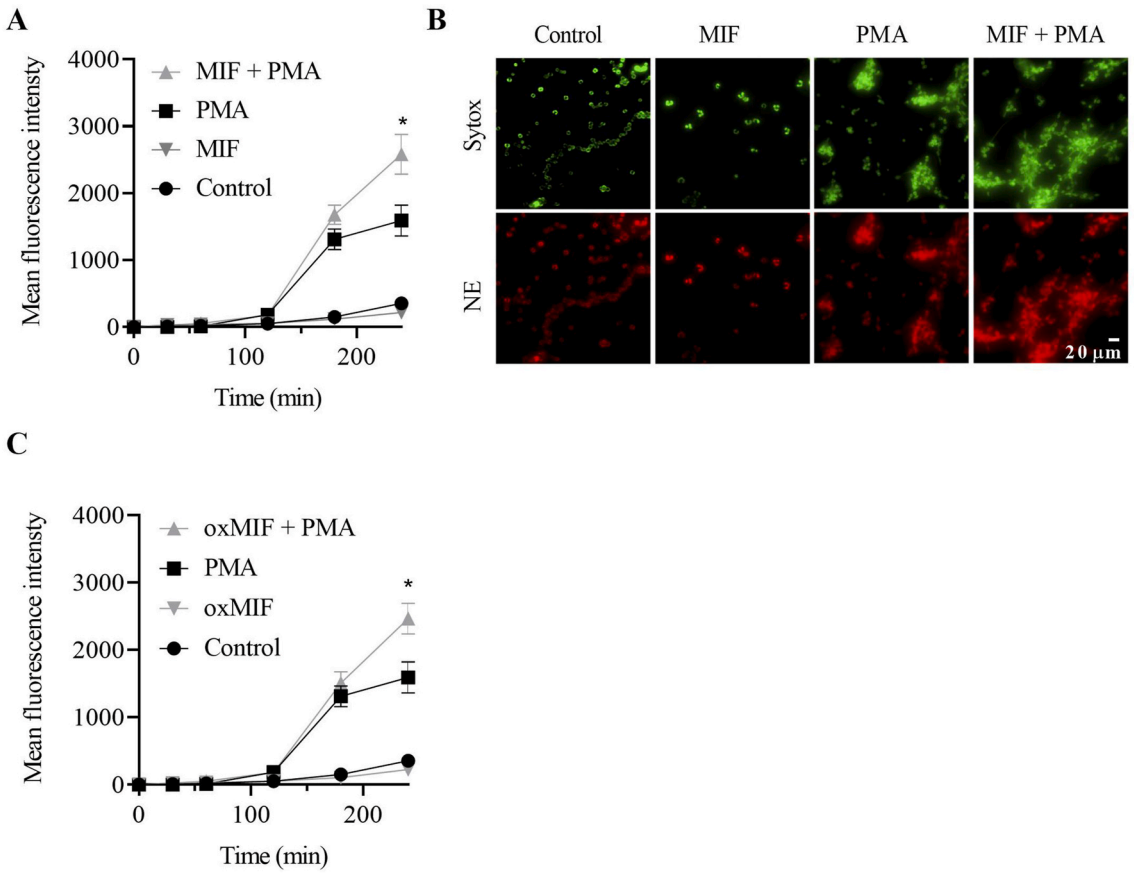

Fig. 8. MIF increases PMA-dependent NET formation. (**A**) Neutrophils (1×10^6 cells/ml) were incubated with or without (control) MIF (10 μg/ml) for 4 h. In separate experiments, neutrophils were incubated with MIF for 1 h, then PMA (20 nM) was added and incubated for 4h. Extracellular DNA was measured at indicated time points using SYTOX Green dye. Each data point shows the mean ± SEM of three independent experiments using different blood donors. A statistical difference between MIF + PMA and PMA was determined using a repeated measures two-way ANOVA with Sidak's multiple comparison test and is indicated by *$p<0.05$. **(B)** After 4 h, neutrophils were fixed on coverslips with paraformaldehyde and stained with SYTOX Green and antibodies against neutrophil elastase (NE) as described in Material and Methods. Representative immunofluorescence microscopy images of two independent experiments are shown. **(C)** Neutrophils were incubated with or without (control) oxMIF (10 μg/ml) for 4 h and extracellular DNA was measured as in (A). (For interpretation of the references to colour in this figure legend, the reader is referred to the Web version of this article.)

[52]. Significant effects of MIF on fMLP-induced superoxide production were observed at concentrations as low as 10 ng/ml. Under physiological conditions, circulating MIF levels are between 2 and 10 ng/ml [1,24,25,73]. However, under disease-related conditions MIF is typically found at a dose range of 25–200 ng/ml highlighting the physiological relevance of the MIF priming effect.

While the cytochrome C assay can be used to accurately measure superoxide released in response to soluble stimuli that trigger extracellular oxidant production, it cannot be used to quantify intra-phagosomal superoxide production. To assess the oxidative burst during phagocytosis, oxidant-sensitive fluorescent and chemiluminescent dyes are often employed [74]. Among them are rhodamine and luminol, which were used to demonstrate an increased oxidant production in neutrophils following MIF exposure [53,54]. The limitations of these probes are that they are not quantitative and cannot report on a specific oxidant [74]. In the present study we assessed the effect of MIF on HOCl generation in phagocytic neutrophils using two independent methods recently described as specific monitoring tools for this oxidant [36,62]. Both the oxidation of bacterial glutathione and R19-S to glutathione sulfonamide and fluorescent R19, assessed by LC-MS and flow cytometry, respectively, demonstrated that the increased oxidative burst hitherto observed in MIF-treated neutrophils was accompanied by an increase in the production of the most toxic oxidant HOCl. R19 and glutathione sulfonamide have already informed on diminished HOCl production in neutrophils from patients with cystic fibrosis [36,75], but they have not previously been used to measure an increase in HOCl generation. Thus, the current work further highlights the utility of R19 and bacterial glutathione sulfonamide as specific HOCl-monitoring tools to evaluate priming.

The first study to observe increased superoxide production in MIF-treated neutrophils also reported that this effect was diminished when the catalytic *N*-terminal proline of MIF was mutated to glycine [52]. Therefore, it was assumed that the priming activity of MIF depended on its tautomerase activity and hence a substrate. In contrast, when we treated MIF with HOCl to oxidize the *N*-terminal to a proline-imine, which abolishes tautomerase activity [66], oxidant production in neutrophils was boosted to the same extent as for untreated MIF. Oxidized MIF was also shown to retain its ability to induce cytokine production in monocytes and to delay neutrophil apoptosis [30]. However, a large number of studies, including the present one, have shown that targeting the *N*-terminal proline with small molecule inhibitors interferes with biological activities of MIF [18,76–78]. Consequently, while enzymatic activity as such seems dispensable for MIF function, a conformational change around the active site proline, following small molecule docking or mutation, must inhibit its interaction with effector cells. In fact, this mechanism has been proposed to affect the binding of MIF to CD74 and the C-X-C chemokine receptor CXCR4 [79,80].

MIF exerts its biological functions through binding of cell surface receptors including CD74, which is not expressed on neutrophils, and the C-X-C chemokine receptors CXCR2, CXCR4 and CXCR7 [26,81,82].

The chemoattractant and anti-apoptotic effect of MIF on neutrophils are known to depend on CXCR2 [26,30] and CXCR4 and MIF were recently shown to be required for NET formation in response to plasmodium-infected erythrocytes [83]. Interestingly, elevated CXCR4 expression in aging neutrophils was shown to coincide with an increased oxidative burst [84]. Furthermore, CXCR4 was shown to regulate NOX2 activity in prostate cancer cells [85]. In light of these studies, the C-X-C chemokine receptors make attractive candidates for further investigations aimed at identifying the cellular cue for the priming effect of MIF on neutrophils.

An interesting finding of the present study is that MIF can potentiate oxidant production in response to all of the investigated stimuli, which act through a variety of pathways. The bacterial peptide fMLP and opsonized zymosan signal through formyl and complement (FCγ)/antibody receptors, which activate different signalling cascades involving phospholipase A_2 (PLA_2) and protein kinase C (PKC), respectively, while the non-physiological stimulus PMA, activates PKC directly [86]. Our finding is in contrast to other reports showing that inflammatory mediators prime the fMLP-mediated oxidative burst, but not that induced by PMA [87–89]. This raises the question as to what molecular mechanism underlies MIF priming. Known priming mechanisms include modulation of the number and affinity of cell surface receptors for the activating stimulus [90], rearrangement of G-proteins in the plasma membrane for more enhanced coupling to activating receptors [91] and structural alterations to NOX2 components [86]. The fact that MIF can prime the receptor-independent activation by PMA points to NOX2 as the site of modulation. In the active, fully assembled state, NOX2 contains a *trans*-membrane flavocytochrome (b_{558} consisting of $p22^{phox}$ and $gp91^{phox}$), a cytosolic part (consisting of $p47^{phox}$, $p67^{phox}$, $p40^{phox}$) and a GTPase (Rac1 or Rac2) [86]. The majority of flavocytochrome b_{558} stems from the membranes of specific granules, which fuse with the plasma membrane upon activation to facilitate extracellular oxidant production or subsequently become part of the phagosomal membrane sealing around an ingested pathogen. Full NOX2 activation then requires phosphorylation of phox subunits, translocation of the cytosolic components to the membrane and GTPase activation [86,92]. Priming agents can cause partial phosphorylation of $p47^{phox}$, induce granule exocytosis and thus flavocytochrome b_{558} mobilisation to the membrane through regulating actin cytoskeleton reorganisation and recruit cytosolic NOX2 components to the plasma membrane [92,93]. These processes are known to be under the control of ERK1/2 and/or p38 MAPK. MIF was shown to promote ERK1/2 phosphorylation in neutrophils and might therefore exert its priming activity in this manner [53]. Because $p47^{phox}$ and $p67^{phox}$ are also phosphorylated during priming by GM-CSF and TNF-α without affecting PMA-stimulated superoxide release, this mechanism is unlikely to entirely account for MIF priming. The fact that MIF not only increased the rate of superoxide production in response to both fMLP and PMA, but also decreased the lag time that is unique to activation by PMA (possibly due to slow membrane penetration), may indicate that MIF may recruit flavocytochrome b_{558} and/or other NOX2 components to the plasma membrane. The exact mechanism that underwrites MIF priming warrants further investigation.

While priming contributes to effective elimination of pathogens, it can also lead to tissue damage and contribute to inflammation through the excessive release of damaging oxidants. Neutrophils with an increased oxidative burst capacity have been isolated from patients with sepsis, ARDS and rheumatoid arthritis [94–96]—all diseases in which a disease-exacerbating role for MIF has been established. The ability to prime oxidant production in neutrophils may therefore contribute to the pro-inflammatory profile of MIF. It remains to be investigated whether oxidant production is potentiated in neutrophils following MIF exposure when they are stimulated by endogenous activators of extracellular oxidant production (e.g. DAMPs, PAF, LTB_4 or C5a) in a setting relevant to sterile inflammation.

The enhanced capacity of MIF-treated neutrophils to generate superoxide in response to PMA observed in the present study coincided with an enhanced PMA-mediated production of NETs. Most inducers of NETs depend on NOX2 activity, but the requirement for MPO varies [55]. PMA requires the activity of both enzymes as evidenced by studies involving patients with non-functional NOX2 (i.e. in chronic granulomatous disease) and MPO-deficiency [97,98]. The present study suggests that PMA-induced NETosis can be boosted by MIF to above the levels observed with healthy neutrophils, presumably as a result of increased oxidant production in MIF-treated neutrophils. Given that oxidant-dependency differs among NET-inducing agents, it will be of interest to investigate whether our finding is limited to PMA-mediated NET formation. A recent study showed that MIF, but not reactive oxygen species, were required for NET formation in response to Plasmodium-infected erythrocytes, suggesting that MIF can affect NET formation via oxidant-independent mechanisms [83]. Priming of neutrophils towards NET formation has previously been observed for G-CSF and was associated with increased tumor growth in a murine model of Lewis lung carcinoma [99]. An analogous mechanism might contribute to MIF's tumorigenic properties. NETs play a role not only cancer, but also in ARDS and cardiovascular disease [58–60] and may thus present a mechanistic link between high levels of MIF observed in these diseases and poor disease outcomes.

In conclusion, this study reports on the ability of MIF to prime HOCl production in phagocytic neutrophils, which adds an important mechanistic facet to the spectrum of biological activities of this atypical cytokine. Our work suggests a role for MIF in enhancing neutrophil killing of bacteria. Future studies should be aimed at understanding whether MIF plays an integral part in enhancing this host defense mechanism *in vivo,* and whether this mechanism plays a role in sterile inflammatory diseases.

Funding

This study was supported by the Canterbury Medical Research Foundation, New Zealand (Grant 04/2018) and the Health Research Council of New Zealand (15/479). L.S. acknowledges travel support from German Academic Exchange Service (DAAD) and the Deutsche Forschungsgemeinschaft (DFG) under Germany's Excellence Strategy within the framework of the Munich Cluster for Systems Neurology (EXC 2145 SyNergy – ID 390857198). L.C.D.S was funded with a Wrightson Postdoctoral Fellowship by the Neurological Foundation of New Zealand (1846WF). J.B. received support from DFG grant SFB1123/A3, from DFG under Germany's Excellence Strategy LMUexc strategic partnership program, and from the Deutsche Zentrum für Herzkreislauf-Forschung (DZHK)/Munich Heart Alliance (MHA) (DZHK B Säule B-Projekt FKZ 81X2600258).

Author contributions

L.S. and N.D. performed the experiments. N.D. wrote the manuscript with input from L.S. and J.B. M.H. and J.B. gave input into conceptual design, helped with interpretation of results, and provided funding. L.C. D.S. assisted with the live cell microscopy experiments. All authors gave scholarly input into the manuscript and approved its final version.

Declaration of competing interest

J.B. is an inventor on patents covering anti-MIF strategies. The other authors declare no conflict of interest.

Acknowledgements

We thank Dr Louisa Ashby for synthesizing R19-S, Judy McKenzie for her assistance with the flow cytometry analyses, and all the blood donors.

Appendix A. Supplementary data

Supplementary data to this article can be found online at https://doi.org/10.1016/j.redox.2021.101946.

References

[1] T. Calandra, T. Roger, Macrophage migration inhibitory factor: a regulator of innate immunity, Nat. Rev. Immunol. 3 (10) (2003) 791–800.
[2] B.R. Bloom, B. Bennett, Mechanism of a reaction in vitro associated with delayed-type hypersensitivity, Science 153 (3731) (1966) 80–82.
[3] J.R. David, Delayed hypersensitivity in vitro: its mediation by cell-free substances formed by lymphoid cell-antigen interaction, Proc. Natl. Acad. Sci. U. S. A. 56 (1) (1966) 72–77.
[4] T. Calandra, et al., MIF as a glucocorticoid-induced modulator of cytokine production, Nature 377 (6544) (1995) 68–71.
[5] K. Meyer-Siegler, Macrophage migration inhibitory factor increases MMP-2 activity in DU-145 prostate cells, Cytokine 12 (7) (2000) 914–921.
[6] J. Chesney, et al., An essential role for macrophage migration inhibitory factor (MIF) in angiogenesis and the growth of a murine lymphoma, Mol. Med. 5 (3) (1999) 181–191.
[7] X. Xu, et al., Overexpression of macrophage migration inhibitory factor induces angiogenesis in human breast cancer, Canc. Lett. 261 (2) (2008) 147–157.
[8] Y.M. Xue, et al., Macrophage migration inhibitory factor promotes cardiac fibroblast proliferation through the Src kinase signaling pathway, Mol. Med. Rep. 17 (2) (2018) 3425–3431.
[9] A. Kapurniotu, O. Gokce, J. Bernhagen, The multitasking potential of alarmins and atypical chemokines, Front. Med. 6 (2019) 3.
[10] E. Rosengren, et al., The macrophage migration inhibitory factor MIF is a phenylpyruvate tautomerase, FEBS Lett. 417 (1) (1997) 85–88.
[11] T. Calandra, et al., The macrophage is an important and previously unrecognized source of macrophage migration inhibitory factor, J. Exp. Med. 179 (6) (1994) 1895–1902.
[12] A. Daryadel, et al., Apoptotic neutrophils release macrophage migration inhibitory factor upon stimulation with tumor necrosis factor-alpha, J. Biol. Chem. 281 (37) (2006) 27653–27661.
[13] K. Imamura, et al., Identification and immunohistochemical localization of macrophage migration inhibitory factor in human kidney, Biochem. Mol. Biol. Int. 40 (6) (1996) 1233–1242.
[14] J. Nishihira, Y. Koyama, Y. Mizue, Identification of macrophage migration inhibitory factor (MIF) in human vascular endothelial cells and its induction by lipopolysaccharide, Cytokine 10 (3) (1998) 199–205.
[15] L. Verschuren, et al., Up-regulation and coexpression of MIF and matrix metalloproteinases in human abdominal aortic aneurysms, Antioxidants Redox Signal. 7 (9–10) (2005) 1195–1202.
[16] J. Bernhagen, et al., MIF is a pituitary-derived cytokine that potentiates lethal endotoxaemia, Nature 365 (6448) (1993) 756–759.
[17] M.S. Basile, et al., The dichotomic role of macrophage migration inhibitory factor in neurodegeneration, Int. J. Mol. Sci. 21 (8) (2020).
[18] J.B. Bilsborrow, et al., Macrophage migration inhibitory factor (MIF) as a therapeutic target for rheumatoid arthritis and systemic lupus erythematosus, Expert Opin. Ther. Targets 23 (9) (2019) 733–744.
[19] K.N. Lai, et al., Role for macrophage migration inhibitory factor in acute respiratory distress syndrome, J. Pathol. 199 (4) (2003) 496–508.
[20] B.J. Plant, et al., Cystic fibrosis, disease severity, and a macrophage migration inhibitory factor polymorphism, Am. J. Respir. Crit. Care Med. 172 (11) (2005) 1412–1415.
[21] C. O'Reilly, et al., Targeting MIF in cancer: therapeutic strategies, current developments, and future opportunities, Med. Res. Rev. 36 (3) (2016) 440–460.
[22] A. Zernecke, J. Bernhagen, C. Weber, Macrophage migration inhibitory factor in cardiovascular disease, Circulation 117 (12) (2008) 1594–1602.
[23] J. Bloom, S. Sun, Y. Al-Abed, MIF, a controversial cytokine: a review of structural features, challenges, and opportunities for drug development, Expert Opin. Ther. Targets 20 (12) (2016) 1463–1475.
[24] I. Kang, R. Bucala, The immunobiology of MIF: function, genetics and prospects for precision medicine, Nat. Rev. Rheumatol. 15 (7) (2019) 427–437.
[25] D. Sinitski, et al., Macrophage migration inhibitory factor (MIF)-Based therapeutic concepts in atherosclerosis and inflammation, Thromb. Haemostasis 119 (4) (2019) 553–566.
[26] J. Bernhagen, et al., MIF is a noncognate ligand of CXC chemokine receptors in inflammatory and atherogenic cell recruitment, Nat. Med. 13 (5) (2007) 587–596.
[27] L.L. Santos, et al., Macrophage migration inhibitory factor regulates neutrophil chemotactic responses in inflammatory arthritis in mice, Arthritis Rheum. 63 (4) (2011) 960–970.
[28] I. Galvao, et al., Macrophage migration inhibitory factor drives neutrophil accumulation by facilitating IL-1beta production in a murine model of acute gout, J. Leukoc. Biol. 99 (6) (2016) 1035–1043.
[29] R. Baumann, et al., Macrophage migration inhibitory factor delays apoptosis in neutrophils by inhibiting the mitochondria-dependent death pathway, Faseb. J. 17 (15) (2003) 2221–2230.
[30] L. Schindler, et al., Macrophage migration inhibitory factor inhibits neutrophil apoptosis by inducing cytokine release from mononuclear cells, J. Leukoc. Biol. (2021), https://doi.org/10.1002/JLB.3A0420-242RRR.
[31] J.H. Oved, et al., Neutrophils promote clearance of nuclear debris following acid-induced lung injury, Blood 137 (3) (2021) 392–397.
[32] J. Wang, et al., Visualizing the function and fate of neutrophils in sterile injury and repair, Science 358 (6359) (2017) 111–116.
[33] M.B. Hampton, A.J. Kettle, C.C. Winterbourn, Inside the neutrophil phagosome: oxidants, myeloperoxidase, and bacterial killing, Blood 92 (9) (1998) 3007–3017.
[34] C.C. Winterbourn, et al., Modeling the reactions of superoxide and myeloperoxidase in the neutrophil phagosome: implications for microbial killing, J. Biol. Chem. 281 (52) (2006) 39860–39869.
[35] J.E. Harrison, J. Schultz, Studies on the chlorinating activity of myeloperoxidase, J. Biol. Chem. 251 (5) (1976) 1371–1374.
[36] N. Dickerhof, et al., Exposure of Pseudomonas aeruginosa to bactericidal hypochlorous acid during neutrophil phagocytosis is compromised in cystic fibrosis, J. Biol. Chem. 294 (36) (2019) 13502–13514.
[37] H.A. Parker, et al., Mycobacterium smegmatis resists the bactericidal activity of hypochlorous acid produced in neutrophil phagosomes, J. Immunol. (2021), https://doi.org/10.4049/jimmunol.2001084.
[38] Y.H. Atkinson, et al., Recombinant human tumor necrosis factor-alpha. Regulation of N-formylmethionylleucylphenylalanine receptor affinity and function on human neutrophils, J. Clin. Invest. 81 (3) (1988) 759–765.
[39] C. Elbim, et al., Differential priming effects of proinflammatory cytokines on human neutrophil oxidative burst in response to bacterial N-formyl peptides, Infect. Immun. 62 (6) (1994) 2195–2201.
[40] A. Ferrante, et al., Effects of tumour necrosis factor alpha and interleukin-1 alpha and beta on human neutrophil migration, respiratory burst and degranulation, Int. Arch. Allergy Appl. Immunol. 86 (1) (1988) 82–91.
[41] R.H. Weisbart, et al., Human granulocyte-macrophage colony-stimulating factor is a neutrophil activator, Nature 314 (6009) (1985) 361–363.
[42] F.R. DeLeo, et al., Neutrophils exposed to bacterial lipopolysaccharide upregulate NADPH oxidase assembly, J. Clin. Invest. 101 (2) (1998) 455–463.
[43] K. Makni-Maalej, et al., The TLR7/8 agonist CL097 primes N-Formyl-Methionyl-Leucyl-Phenylalanine-Stimulated NADPH oxidase activation in human neutrophils: critical role of p47phox phosphorylation and the proline isomerase Pin1, J. Immunol. 189 (9) (2012) 4657–4665.
[44] F. Hayashi, T.K. Means, A.D. Luster, Toll-like receptors stimulate human neutrophil function, Blood 102 (7) (2003) 2660–2669.
[45] R.H. Daniels, et al., Priming of the oxidative burst in human neutrophils by physiological agonists or cytochalasin B results from the recruitment of previously non-responsive cells, Immunology 82 (3) (1994) 465–472.
[46] L.C. McPhail, C.C. Clayton, R. Snyderman, The NADPH oxidase of human polymorphonuclear leukocytes. Evidence for regulation by multiple signals, J. Biol. Chem. 259 (9) (1984) 5768–5775.
[47] H. Mossmann, et al., Effect of platelet-activating factor on human polymorphonuclear leukocyte enhancement of chemiluminescence and antibody-dependent cellular cytotoxicity, J. Leukoc. Biol. 39 (2) (1986) 153–165.
[48] B.A. Walker, P.A. Ward, Priming and signal transduction in neutrophils, Biol. Signals 1 (5) (1992) 237–249.
[49] C. Guichard, et al., Interleukin-8-induced priming of neutrophil oxidative burst requires sequential recruitment of NADPH oxidase components into lipid rafts, J. Biol. Chem. 280 (44) (2005) 37021–37032.
[50] M.D. Wewers, et al., Tumor necrosis factor infusions in humans prime neutrophils for hypochlorous acid production, Am. J. Physiol. 259 (4 Pt 1) (1990) L276–L282.
[51] A.F. Lopez, et al., Recombinant human granulocyte-macrophage colony-stimulating factor stimulates in vitro mature human neutrophil and eosinophil function, surface receptor expression, and survival, J. Clin. Invest. 78 (5) (1986) 1220–1228.
[52] M. Swope, et al., Direct link between cytokine activity and a catalytic site for macrophage migration inhibitory factor, EMBO J. 17 (13) (1998) 3534–3541.
[53] M. Dwyer, et al., Cystic fibrosis sputum DNA has NETosis characteristics and neutrophil extracellular trap release is regulated by macrophage migration-inhibitory factor, J Innate Immun 6 (6) (2014) 765–779.
[54] J. Hao, et al., Macrophage migration inhibitory factor contributes to anti-neutrophil cytoplasmic antibody-induced neutrophils activation, Hum. Immunol. 77 (12) (2016) 1209–1214.
[55] H. Parker, C.C. Winterbourn, Reactive oxidants and myeloperoxidase and their involvement in neutrophil extracellular traps, Front. Immunol. 3 (2012) 424.
[56] B. Fadeel, et al., Involvement of caspases in neutrophil apoptosis: regulation by reactive oxygen species, Blood 92 (12) (1998) 4808–4818.
[57] C. Dahlgren, A. Karlsson, J. Bylund, Intracellular neutrophil oxidants: from laboratory curiosity to clinical reality, J. Immunol. 202 (11) (2019) 3127–3134.
[58] E.A. Middleton, et al., Neutrophil extracellular traps contribute to immunothrombosis in COVID-19 acute respiratory distress syndrome, Blood 136 (10) (2020) 1169–1179.
[59] M. Garley, E. Jablonska, D. Dabrowska, NETs in cancer, Tumour Biol 37 (11) (2016) 14355–14361.
[60] A. Bonaventura, et al., Neutrophil extracellular traps and cardiovascular diseases: an update, Cells 9 (1) (2020).
[61] D.T. Harwood, A.J. Kettle, C.C. Winterbourn, Production of glutathione sulfonamide and dehydroglutathione from GSH by myeloperoxidase-derived oxidants and detection using a novel LC-MS/MS method, Biochem. J. 399 (1) (2006) 161–168.
[62] A.M. Albrett, et al., Heterogeneity of hypochlorous acid production in individual neutrophil phagosomes revealed by a rhodamine-based probe, J. Biol. Chem. 293 (40) (2018) 15715–15724.
[63] X. Chen, et al., Synthesis of a highly HOCl-selective fluorescent probe and its use for imaging HOCl in cells and organisms, Nat. Protoc. 11 (7) (2016) 1219–1228.

[64] J.C. Morris, Acid ionization constant of HOCl from 5 to 35 degrees, J. Phys. Chem. 70 (12) (1966) 3798–3805.
[65] A.W. Segal, J. Dorling, S. Coade, Kinetics of fusion of the cytoplasmic granules with phagocytic vacuoles in human polymorphonuclear leukocytes. Biochemical and morphological studies, J. Cell Biol. 85 (1) (1980) 42–59.
[66] N. Dickerhof, et al., Macrophage migration inhibitory factor (MIF) is rendered enzymatically inactive by myeloperoxidase-derived oxidants but retains its immunomodulatory function, Free Radic. Biol. Med. 89 (2015) 498–511.
[67] N. Dickerhof, et al., Potent inhibition of macrophage migration inhibitory factor (MIF) by myeloperoxidase-dependent oxidation of epicatechins, Biochem. J. 462 (2) (2014) 303–314.
[68] A.K. Gupta, et al., Induction of neutrophil extracellular DNA lattices by placental microparticles and IL-8 and their presence in preeclampsia, Hum. Immunol. 66 (11) (2005) 1146–1154.
[69] M.F. Leyton-Jaimes, J. Kahn, A. Israelson, AAV2/9-mediated overexpression of MIF inhibits SOD1 misfolding, delays disease onset, and extends survival in mouse models of ALS, Proc. Natl. Acad. Sci. U. S. A. 116 (29) (2019) 14755–14760.
[70] P. Luedike, et al., Cardioprotection through S-nitros(yl)ation of macrophage migration inhibitory factor, Circulation 125 (15) (2012) 1880–1889.
[71] K.J. Filbey, et al., Macrophage migration inhibitory factor (MIF) is essential for type 2 effector cell immunity to an intestinal helminth parasite, Front. Immunol. 10 (2019) 2375.
[72] A.L. Chapman, et al., Chlorination of bacterial and neutrophil proteins during phagocytosis and killing of Staphylococcus aureus, J. Biol. Chem. 277 (12) (2002) 9757–9762.
[73] J. Sobierajski, et al., Assessment of macrophage migration inhibitory factor in humans: protocol for accurate and reproducible levels, Free Radic. Biol. Med. 63 (2013) 236–242.
[74] C.C. Winterbourn, The challenges of using fluorescent probes to detect and quantify specific reactive oxygen species in living cells, Biochim. Biophys. Acta 1840 (2) (2014) 730–738.
[75] H.P. Ng, V.G. Valentine, G. Wang, CFTR targeting during activation of human neutrophils, J. Leukoc. Biol. 100 (6) (2016) 1413–1424.
[76] Y. Al-Abed, S. VanPatten, MIF as a disease target: ISO-1 as a proof-of-concept therapeutic, Future Med. Chem. 3 (1) (2011) 45–63.
[77] H. Ouertatani-Sakouhi, et al., Identification and characterization of novel classes of macrophage migration inhibitory factor (MIF) inhibitors with distinct mechanisms of action, J. Biol. Chem. 285 (34) (2010) 26581–26598.
[78] D. Rajasekaran, et al., Targeting distinct tautomerase sites of D-DT and MIF with a single molecule for inhibition of neutrophil lung recruitment, Faseb. J. 28 (11) (2014) 4961–4971.
[79] G. Pantouris, et al., An analysis of MIF structural features that control functional activation of CD74, Chem. Biol. 22 (9) (2015) 1197–1205.
[80] D. Rajasekaran, et al., Macrophage migration inhibitory factor-CXCR4 receptor interactions: evidence for partial allosteric agonism IN comparison with CXCL12 chemokine, J. Biol. Chem. 291 (30) (2016) 15881–15895.
[81] S. Alampour-Rajabi, et al., MIF interacts with CXCR7 to promote receptor internalization, ERK1/2 and ZAP-70 signaling, and lymphocyte chemotaxis, Faseb. J. 29 (11) (2015) 4497–4511.
[82] L. Leng, et al., MIF signal transduction initiated by binding to CD74, J. Exp. Med. 197 (11) (2003) 1467–1476.
[83] D.A.S. Rodrigues, et al., CXCR4 and MIF are required for neutrophil extracellular trap release triggered by Plasmodium-infected erythrocytes, PLoS Pathog. 16 (8) (2020), e1008230.
[84] D. Zhang, et al., Neutrophil ageing is regulated by the microbiome, Nature 525 (7570) (2015) 528–532.
[85] K.J. Jones, et al., Cysteine (C)-X-C Receptor 4 Regulates NADPH Oxidase-2 during Oxidative Stress in Prostate Cancer Cells, Cancer Microenviron, 2013.
[86] F.R. Sheppard, et al., Structural organization of the neutrophil NADPH oxidase: phosphorylation and translocation during priming and activation, J. Leukoc. Biol. 78 (5) (2005) 1025–1042.
[87] S.R. McColl, et al., Priming of the human neutrophil respiratory burst by granulocyte-macrophage colony-stimulating factor and tumor necrosis factor-alpha involves regulation at a post-cell surface receptor level. Enhancement of the effect of agents which directly activate G proteins, J. Immunol. 145 (9) (1990) 3047–3053.
[88] R.H. Weisbart, et al., Human GM-CSF primes neutrophils for enhanced oxidative metabolism in response to the major physiological chemoattractants, Blood 69 (1) (1987) 18–21.
[89] J.C. Gay, et al., Enhancement of chemotactic factor-stimulated neutrophil oxidative metabolism by leukotriene B4, Blood 64 (4) (1984) 780–785.
[90] R.H. Weisbart, D.W. Golde, J.C. Gasson, Biosynthetic human GM-CSF modulates the number and affinity of neutrophil f-Met-Leu-Phe receptors, J. Immunol. 137 (11) (1986) 3584–3587.
[91] M.L. Keil, et al., Priming-induced localization of G(ialpha2) in high density membrane microdomains, Biochem. Biophys. Res. Commun. 301 (4) (2003) 862–872.
[92] G.T. Nguyen, E.R. Green, J. Mecsas, Neutrophils to the ROScue: mechanisms of NADPH oxidase activation and bacterial resistance, Front Cell Infect Microbiol 7 (2017) 373.
[93] J. El-Benna, et al., Priming of the neutrophil respiratory burst: role in host defense and inflammation, Immunol. Rev. 273 (1) (2016) 180–193.
[94] D.A. Bass, et al., Subpopulations of neutrophils with increased oxidative product formation in blood of patients with infection, J. Immunol. 136 (3) (1986) 860–866.
[95] S. Chollet-Martin, et al., Subpopulation of hyperresponsive polymorphonuclear neutrophils in patients with adult respiratory distress syndrome. Role of cytokine production, Am. Rev. Respir. Dis. 146 (4) (1992) 990–996.
[96] H.L. Nurcombe, R.C. Bucknall, S.W. Edwards, Neutrophils isolated from the synovial fluid of patients with rheumatoid arthritis: priming and activation in vivo, Ann. Rheum. Dis. 50 (3) (1991) 147–153.
[97] K.D. Metzler, et al., Myeloperoxidase is required for neutrophil extracellular trap formation: implications for innate immunity, Blood 117 (3) (2011) 953–959.
[98] T.A. Fuchs, et al., Novel cell death program leads to neutrophil extracellular traps, J. Cell Biol. 176 (2) (2007) 231–241.
[99] M. Demers, et al., Priming of neutrophils toward NETosis promotes tumor growth, OncoImmunology 5 (5) (2016), e1134073.